

Influence of Infill Structures and Process Parameters on the Tensile Strength of 3D-printed PEEK Parts

Christoph Rehekampff, Andreas Schroeffler, Franz Irlinger and Tim C. Lueth, *Senior Member IEEE*

Institute of Micro Technology and Medical Device Technology

Technical University of Munich

Boltzmannstr. 15, 85748 Garching, Germany

christoph.rehekampff@tum.de

Abstract - Polyetheretherketone (PEEK) is a high performance semi crystalline polymer used in technical applications as well as for medical purposes. Its mechanical properties and its temperature resistance often allow its use instead of metal for lightweight applications. In the medical field, its biocompatibility and the modulus of elasticity similar to this of bones make it a good choice for implants. For this purpose, additive manufacturing is a technology that allows the economic production of patient-specific implants. Until now, only few 3D-printers for PEEK are available on the market and only few process knowledge is available so far. In this paper, PEEK parts are fabricated using a 3D-printer based on the Fused Layer Manufacturing (FLM) technology. The influence of different process parameters on the mechanical properties of the specimens is investigated. For this, printing speed, local part cooling, filling degree and infill geometry are varied and the tensile strength of the corresponding specimens is investigated. Fracture surfaces are analyzed using optical microscopy and scanning electron microscopy. Results show a slightly increase of tensile strength at lower printing speed. Filling degree as expected has great influence on the mechanical properties. Optical investigation often shows insufficient adhesion between the single layers. Also a filament with carbon fiber reinforcement is used and compared to the standard material. This material shows a significant increase in tensile strength and stiffness.

Index Terms – Additive Manufacturing, 3D-Printing, PEEK, Fused Layer Manufacturing.

I. INTRODUCTION

During the last years, additive manufacturing technologies have become increasingly important. Besides prototyping, additive manufacturing allows the economic production of small series and individual pieces. Production costs are in principle independent of the part's complexity. Therefore, even complex geometries such as patient-specific implants can be realized easily. In order to design a part appropriate to the load case during its use, it is necessary to have knowledge about the mechanical properties of the parts produced by additive manufacturing.

A. Extrusion-based Additive Manufacturing

Additive manufacturing methods can be categorized into seven groups according to the standard DIN EN ISO / ASTM 52900. One of them is *material extrusion*, of which Fused Deposition Modeling (FDM) is probably the best known technology. This process, originally developed by Stratasys (*Stratasys Ltd.*) is also known as Fused Filament Fabrication

(FFF) or Fused Layer Manufacturing (FLM) [1, 2]. In this paper, the term FLM will be used.

In FLM, raw material in form of a filament is extruded by a motor through a heated nozzle. The material is melted in the nozzle and deposited on the building platform in strands layer by layer (Fig. 1). The deposited material is combined with the underlying layer as well as with the adjacent strands by thermal melting. This method is therefore good suitable for materials with a low melting point like polymers and wax [2]. Commonly used polymers are e.g. acrylonitrile butadiene styrene (ABS), polylactic acid (PLA) and acrylonitrile styrene acrylate (ASA) [3].

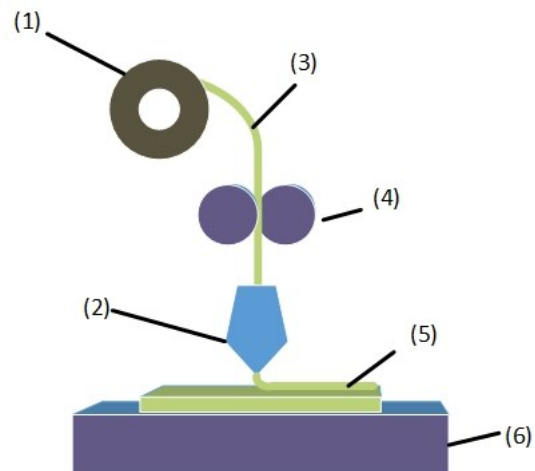


Figure 1: Components of a FLM-printer: (1) filament spool, (2) printhead, (3) filament, (4) extruder, (5) deposited material, (6) heated build platform

The mechanical strength of components manufactured by FLM is comparatively high, but has not yet reached the values of injection molded parts. Due to the fabrication principle, mechanical properties show anisotropic behavior in the form that the parts can withstand loads parallel to the single layers better than loads normal to the layers. [4] To overcome this, new processes are developed such as a droplet-based extrusion process [5].

B. Fabrication of PEEK in FLM

Polymers like ABS and PLA can even be processed in simple and low cost 3D-printers with good results. However, for many applications, polymers with better mechanical properties are needed. Polyetheretherketone (PEEK) is a semi

crystalline polymer that can be used as a replacement for metal parts for example in medical or in aerospace applications due to its good biocompatibility and its high tensile strength [6]. Since PEEK has an modulus of elasticity that is closer to that of human bones than metals, less stress shielding occurs, which leads to a better osseointegration of PEEK implants [7]. Furthermore, PEEK occurs transparent in X-ray images which makes investigations after surgery easier [1]. Another advantage of 3D-printing is that implants can be designed patient-specific at economic costs instead of traditional methods like milling or injection molding [8].

However, 3D-printing of high performance polymers like PEEK brings up new challenges. Due to its high melting point, higher nozzle temperatures are necessary [9]. Furthermore, PEEK is a semi crystalline polymer, that means while cooling and solidification the molecules partially arrange in a highly ordered way. As a result, mechanical properties like tensile strength and stiffness increase at higher crystallinity levels. However, crystallization leads to further shrinkage of the material and can result in warpage of the manufactured parts [10, 11]. To overcome this, a precise temperature management is necessary to guarantee a homogenous temperature across the part and to realize a smooth cooling [9]. This can be achieved by a heated build chamber in addition to a heated build platform. Temperature management during the process has a large influence on interlayer bonding and on crystallinity [9, 12].

In this work, PEEK specimens are fabricated using a high-temperature FLM 3D-printer that allows for a homogenous temperature distribution in the building chamber of up to 200°C using circulating heated air (HTRD 1.0, *Kumovis GmbH*). The printhead is moved by Delta kinematics and can be heated up to 500°C. The build platform consists of a glass plate that can be heated up to a temperature of 300°C. Two air nozzles close to the extruder allow a cooling of the molten material immediately after its deposition. This way, part precision can be increased due to the fast solidification. However, a faster cooling decreases crystallinity and potentially decreases melting of adjacent material strands.

Process parameters such as printing speed, local cooling using the air nozzles, filling degree and infill geometry are varied. Tensile strength of the specimens is measured and fracture surfaces are analyzed using optical microscopy and scanning electron microscopy.

II. EXPERIMENTS

In order to allow for a load-appropriate design of 3D-printed PEEK parts, knowledge about the mechanical properties is needed. Therefore, test specimens for tensile testing according to ISO 527 are produced. Test specimens are designed according to type 1BA with an overall length of 80 mm, while the cross-section in the middle has the dimensions 5 mm x 2 mm.

For all experiments an extruder nozzle with a diameter of 0.4 mm is used. Nozzle temperature is adjusted to 415°C

according to the recommendation of the material manufacturer. Higher temperatures have a benefit on material bonding. However, they can decrease part accuracy by making the material less stiff during its deposition. KetaSpire® AM MS NT1 PEEK filament is used as material (*Solvay Specialty Polymers USA, L.L.C.*). For comparison, some specimens are also produced using carbon-fiber reinforced KetaSpire® HC AM CF10 LS1 PEEK filament (*Solvay Specialty Polymers USA, L.L.C.*). The height of the printed layers is set to 0.2 mm. The heated build has a temperature of 260°C for the first layer to achieve good adhesion. For the following layers, platform temperature is decreased to 210°C. The air temperature in the build chamber around the parts is set to 200-220°C.

Specimens with filling degrees of 25, 50, 75 and 100 % are produced at infill raster angles of +45°/-45° and 0°/90°. Influence of local material cooling is investigated at specimens with 0° infill raster angle and 100 % filling degree. For this, the air temperature of the cooling nozzles is set to 180°C. To determine the influence of printing speed, parts are produced with 0° infill raster angle and 100 % filling degree at printing speeds of 450 mm/min, 900 mm/min (default value) and 1800 mm/min. Carbon-fiber reinforced specimens are produced with a filling degree of 100 % and an infill raster angle of 0°. For each parameter set 3 samples are produced.

Tensile testing is performed using a universal testing machine (Z050, *ZwickRoell GmbH & Co. KG*) with a 50 kN load cell. Specimens are loaded until breaking at a speed of 50 mm/min. The tensile strength and strain are measured and recorded during testing.

After tensile testing fracture surfaces are analyzed using a digital optical microscope (VHX-5000, *Keyence Corporation*) as well as a scanning electron microscope (SEM) (JSM-5500, *JEOL (Germany) GmbH*). This way, failure modes can be analyzed in order to optimize the printing process.

III. RESULTS AND DISCUSSION

In this section, the results of the performed experiments are presented.

A. Filling degree and infill raster angle

Fig. 2 shows a typical stress-strain curve resulting from a tensile testing experiment. At low strain the material shows linear-elastic behavior, while at higher strains plastification occurs and the part finally breaks.

Tensile strength is determined at four different filling degrees using an infill raster angle of +45°/-45° and 0°/90° (Tab. 1, Tab. 2, Fig. 3).

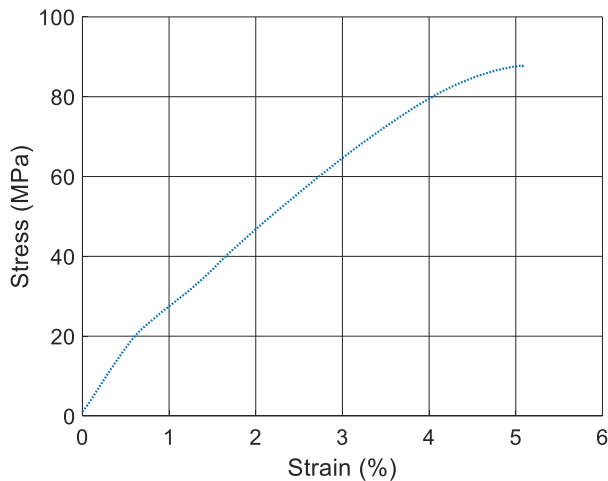


Figure 2: Stress-Strain diagram of a tensile test with a PEEK specimen. Until a stress of 20 MPa / a strain of 0.6 % the material shows linear-elastic behavior. At higher strain, plastification occurs until the part breaks.

TABLE I

MEASURED TENSILE STRENGTH AT DIFFERENT FILLING DEGREES WITH AN INFILL RASTER ANGLE OF $+45^{\circ}/-45^{\circ}$

Filling Degree (%)	Ultimate Tensile Strength (MPa)			Mean Tensile Strength (MPa)
25	37.2	37.8	38.0	37.7
50	42.7	44.2	47.3	44.7
75	50.5	53.9	62.2	55.5
100	85.2	87.8	92.9	88.6

TABLE II

MEASURED TENSILE STRENGTH AT DIFFERENT FILLING DEGREES WITH AN INFILL RASTER ANGLE OF $0^{\circ}/90^{\circ}$

Filling Degree (%)	Ultimate Tensile Strength (MPa)			Mean Tensile Strength (MPa)
25	29.5	32.7	35.2	32.5
50	50.7	59.5	63.1	57.8
75	57.6	70.9	79.3	69.3
100	77.7	81.5	90.9	83.4

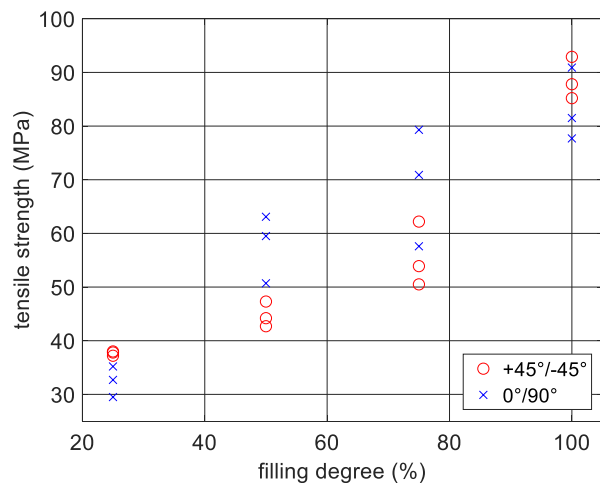


Figure 3: Tensile strength of specimens with infill raster angle of $+45^{\circ}/-45^{\circ}$ and $0^{\circ}/90^{\circ}$ at filling degrees of 25 %, 50 %, 75 % and 100 %.

As expected, tensile strength clearly increases at higher filling degrees. It can be seen that already at filling degrees of 50 % and above, tensile strength of the specimens with raster angle $0^{\circ}/90^{\circ}$ is higher than of those with $+45^{\circ}/-45^{\circ}$. However, when considering the scattering of the measured values, this difference is not significant. The mean value at 100 % filling degree is 88.6 MPa ($+45^{\circ}/-45^{\circ}$) respectively 83.4 MPa ($0^{\circ}/90^{\circ}$). The material datasheet specifies a tensile strength of 85 MPa. So it can be seen, that with the used printing parameters this value can be achieved and therefore the material's potential can be exploited.

B. Microscopic analysis of fracture surfaces

Fig. 4 shows a comparative image of specimens with 100 % filling degree each. (a) and (b) show a specimen with a raster angle of $+45^{\circ}/-45^{\circ}$ like the specimens in Fig. 5. (c) and (d) show a specimen with a raster angle of $0^{\circ}/90^{\circ}$.

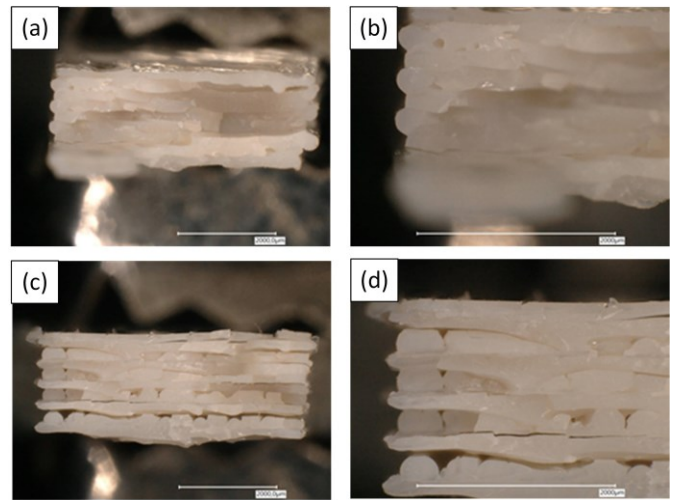


Figure 4: Microscopic images of the fracture surfaces of specimens with a raster angle of $+45^{\circ}/-45^{\circ}$ ((a), (b)) and $0^{\circ}/90^{\circ}$ ((c), (d)) at a filling degree of 100 %. Images in the left column were taken at 50x magnification while in the right column 100x magnification is used.

Insufficient layer-layer bonding especially at the specimen with $0^{\circ}/90^{\circ}$ raster angle can be seen, as the layers are clearly separated from each other. However, as the results of the tensile test show, tensile strength of both specimens are almost identical. Since the load is applied parallel to the single layers, the bad layer-layer bonding is expected not to have large influence on the tensile strength in this direction. For other load directions, a better layer-layer bonding is more crucial.

Fig. 5 shows microscopic images of the fracture surfaces of specimens with a raster angle of $+45^{\circ}/-45^{\circ}$. From top to bottom, the images show specimens with increasing filling degrees (25 %, 50 %, 75 %, 100 %). The left column shows the specimens at a magnification of 50x while in the right column a magnification of 100x is used.

Fig. 6 shows SEM images of the fracture surface of a part after tensile testing.

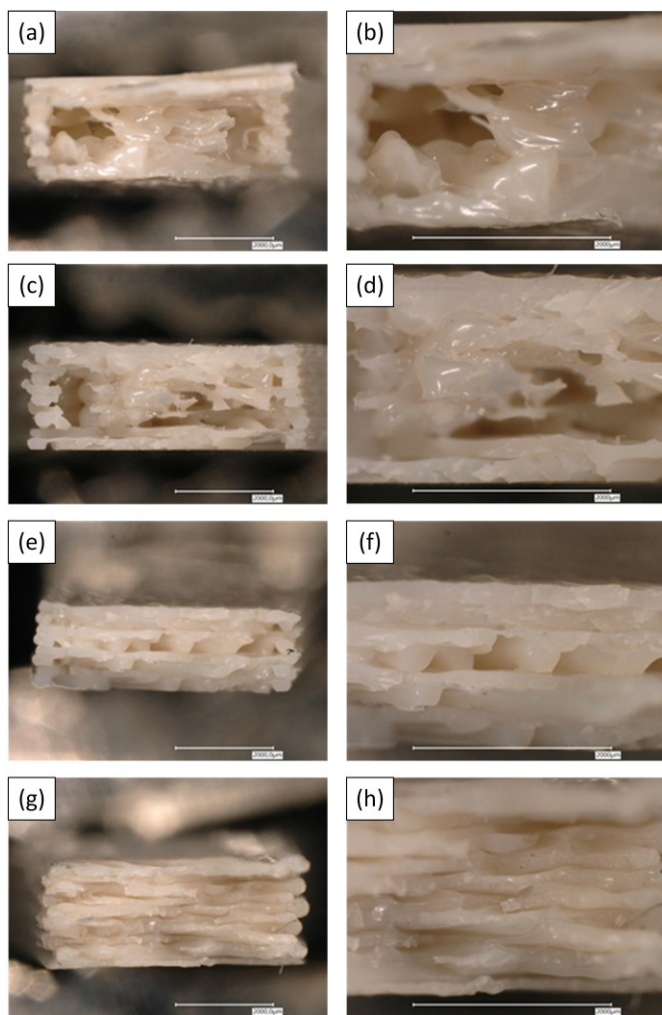


Figure 5: Microscopic images of the fracture surfaces of specimens with a raster angle of $+45^{\circ}/-45^{\circ}$. (a) and (b): 25 % filling degree. (c) and (d): 50 % filling degree. (e) and (f): 75 % filling degree. (g) and (h): 100 % filling degree. The left column shows the specimens at a magnification of 50x, while magnification in the right column is 100x.

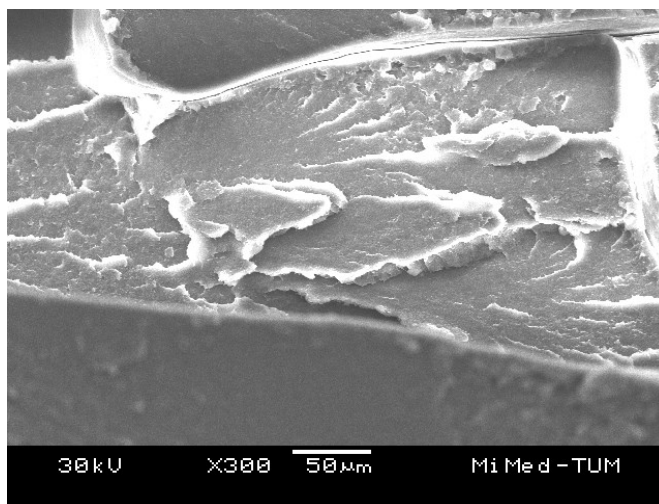
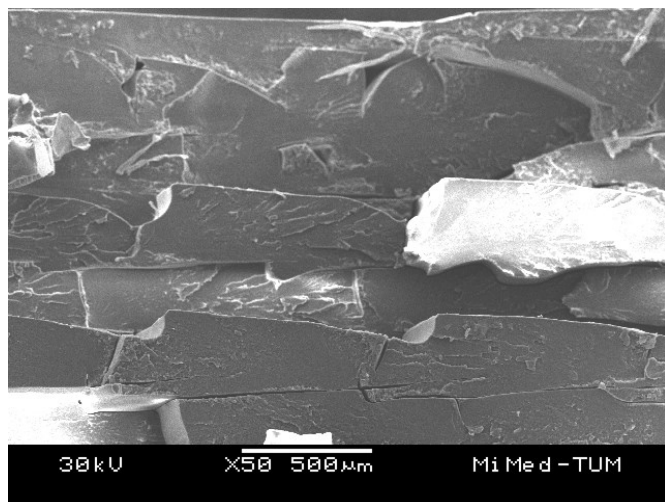


Figure 6: SEM images of the fracture surface of a PEEK part after tensile testing at magnification 50x and 300x. Since the single layers can be clearly identified, this again is an indicator for insufficient layer-layer bonding.

As it can be seen from the images, the single strands and the raster angle of $+45^{\circ}/-45^{\circ}$ are clearly visible. Even at a filling degree of 100 % (images (g) and (h)), some single strands can be seen. Furthermore, the single layers seem not to be well connected since the boundary surfaces between them are clearly visible. So it can be concluded that insufficient melting of the underlying layers is achieved. A higher extrusion temperature might improve this due to better melting of the previously deposited material.

C. Influence of local part cooling

The used 3D-printer has a cooling nozzle that allows for a cooling of the polymer by temperature controlled air directly after its deposition to achieve a fast solidification. While potentially increasing part precision, the fast cooling rate might decrease the bonding to previously deposited material, thus have a negative influence on tensile strength. To investigate the impact on tensile strength, parts with a filling degree of 100 % at a raster angle of 0° (unidirectional) are produced. Tab. 3 and Fig. 7 show the results of this experiment.

TABLE III
TENSILE STRENGTH OF SPECIMENS WITH AND WITHOUT LOCAL COOLING
ENABLED. THE FILLING DEGREE IS 100 % AT A RASTER ANGLE OF 0°

Local Cooling	Ultimate Tensile Strength (MPa)			Mean Tensile Strength (MPa)
On	86.5	90.1	90.7	89.1
Off	84.3	85.1	85.9	85.1

From Fig. 7 and Tab. 3 it can be seen that there is only a small difference in tensile strength between the samples with or without local cooling. The parts with enabled local cooling even show a slightly higher tensile strength, however this is not significant when considering the scattering of the measured values. During the tensile test, the potentially decreased

bonding to the previously deposited material seems not to have a negative influence.

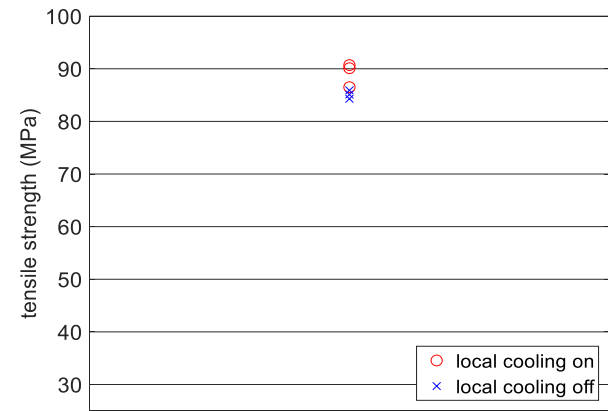


Figure 7: Influence of local cooling on tensile strength. Specimens with a filling degree of 100 % and a raster angle of 0° are produced with and without local cooling. As it can be seen, no significant difference in tensile strength exists when considering the scattering of the measured values.

D. Influence of printing speed

At lower printing speed, the heated nozzle can transfer more heat into the deposited material, thus allowing for a better fusing of the single strands and layers. Tab. 4 and Fig. 8 show the results of specimens printed at different speeds. The default speed used is 900 mm/min. For this experiment, additional specimens are printed with 450 mm/min (50 %) and 1800 mm/min (200 %).

TABLE IV
TENSILE STRENGTH AT DIFFERENT PRINTING SPEEDS WITH A FILLING DEGREE OF 100 % AT A RASTER ANGLE OF 0°

Printing Speed (mm/min)	Ultimate Tensile Strength (MPa)			Mean Tensile Strength (MPa)
450	84.3	90.7	93.2	89.4
900	84.3	85.1	85.9	85.1
1800	69.4	72.0	77.0	72.8

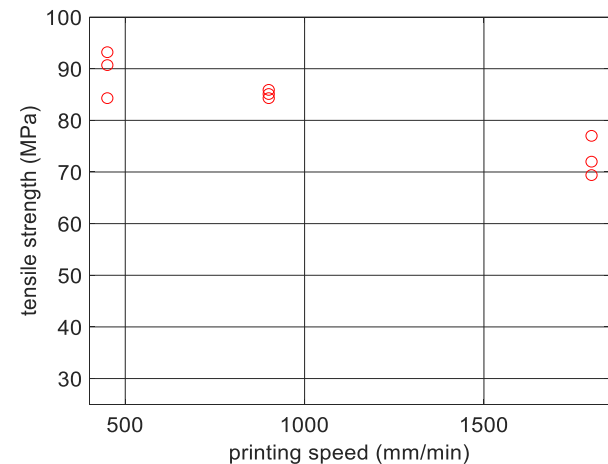


Figure 8: Relationship between printing speed and tensile strength. Specimens are produced at printing speeds of 450 mm/min, 900 mm/min and 1800 mm/min with a filling degree of 100 % at a raster angle of 0°.

As expected, tensile strength decreases with increasing printing speed due to the reduced heat transfer into the material. Increasing speed from 450 mm/min to 900 mm/min has a measurable but not significant influence. However, further increase from 900 mm/min to 1800 mm/min shows a significant decrease of tensile strength. So it can be concluded that the chosen default printing speed of 900 mm/min is a good trade-off regarding strength and print time. Print time can be further reduced by increasing the speed when maximum tensile strength is not necessary.

E. Carbon fiber reinforced material

Fig. 9 and Tab. 5 show the results of a comparison between carbon fiber reinforced filament with 10 % fiber fraction (KetaSpire® HC AM CF10 LS1 PEEK) and standard filament (KetaSpire® AM MS NT1 PEEK), both produced by Solvay (Solvay Specialty Polymers USA, L.L.C.). For this, specimens with 100 % filling degree and a raster angle of 0° are used.

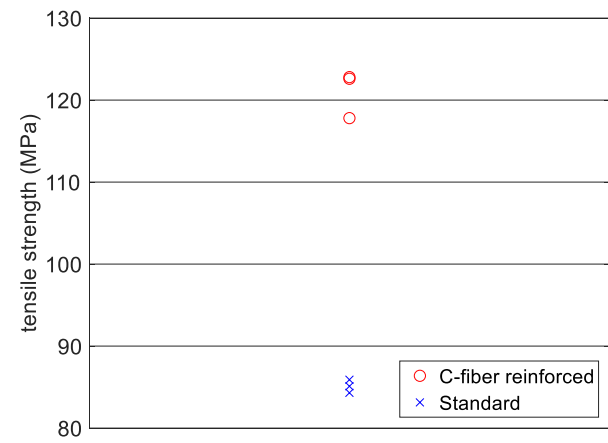


Figure 9: Comparison of carbon fiber reinforced PEEK and standard PEEK. Specimens are printed with a filling degree of 100 % at a raster angle of 0°.

TABLE V
COMPARISON BETWEEN CARBON FIBER REINFORCED PEEK AND STANDARD PEEK. SPECIMENS ARE PRODUCED WITH A FILLING DEGREE OF 100 % AT A RASTER ANGLE OF 0°

Material	Ultimate Tensile Strength (MPa)			Mean Tensile Strength (MPa)
Carbon Fiber	117.8	122.6	122.8	121.1
Standard	84.3	85.1	85.9	85.1

As expected, the reinforced material achieves significant higher (42 %) tensile strength than the standard material. However, in contrast to the standard material, the value given in the material datasheet (144 MPa) is not reached in this experiment. As expected, the material shows a much stiffer behavior and therefore a more brittle fracture behavior.

Fig. 10 shows the fracture surface of a fiber reinforced specimen printed with a filling degree of 100 % at a raster angle of 0°. The carbon fibers are visible as small black particles.

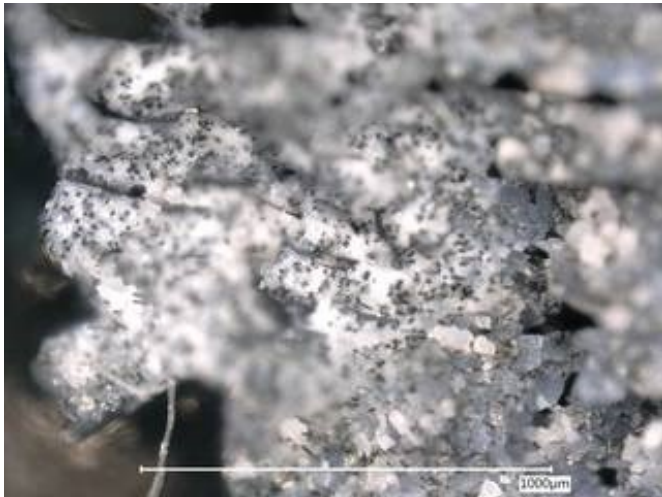


Figure 10: 200x magnified fracture surface of a specimen made of carbon fiber reinforced PEEK. The carbon fibers can be seen as small black parts surrounded by the polymer.

Fig. 11 shows a SEM image of the fiber reinforced specimen. A pulled out fiber (1) as well as a fiber partly surrounded by polymer (3) and a hole where a fiber has been pulled out (2) can be identified. This shows that the fibers itself are stronger than the fiber-polymer interface, since the fibers did not break but were pulled out of the matrix instead.

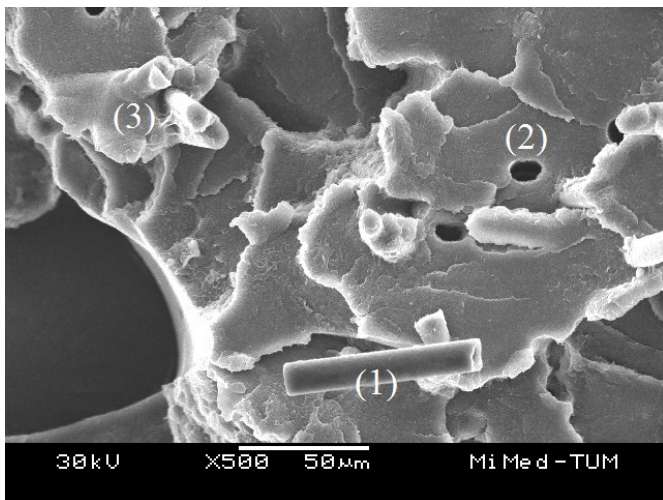


Figure 11: SEM image of the fracture surface at 500x magnification. A single fiber not surrounded by polymer can be seen in the lower area (1). Fibers partly surrounded by polymer (3) as well as holes where fibers have been pulled out (2) can be seen in the upper area of the image.

IV. CONCLUSION

The results show the influence of different processing parameters, filling degrees and infill structures on the tensile strength of PEEK parts produced by additive manufacturing. As expected, filling degree strongly increases tensile strength, while also leading to higher weight and material cost. For a cost optimized part, filling degree can be chosen according to the mechanical load the part has to withstand. Infill raster

angle has only low influence on tensile strength. Optical microscopy and SEM show insufficient layer-layer bonding in most of the parts. This does not influence tensile strength parallel to the layers, but for loads perpendicular to the layers this is expected to be critical. For this, further investigations regarding anisotropy of the mechanical properties need to be done. A higher printing speed, as expected, has negative influence on tensile strength. However, if tensile strength is not critical for certain applications, build time can be significantly reduced by increasing printing speed. For high-load applications, carbon fiber reinforced PEEK is available and shows much higher mechanical strength and stiffness. However, the stiffer material behavior also leads to less flexibility and therefore to a more brittle breaking of the part.

ACKNOWLEDGMENT

The authors would like to thank the Institute of Medical and Polymer Engineering at TUM for making their tensile testing machine available. Further thanks goes out to Vanessa Weisbrodt for her support in conducting the experiments.

REFERENCES

- [1] P. Fastermann, *3D-Drucken: Wie die generative Fertigungstechnik funktioniert*. Springer-Verlag, 2014.
- [2] A. Gebhardt, *Generative Fertigungsverfahren: Rapid Prototyping - Rapid Tooling - Rapid Manufacturing*. Hanser, 2007.
- [3] R. Hagl, *Das 3D-Druck-Kompodium: Leitfaden für Unternehmer, Berater und Innovationstreiber*. Springer Fachmedien Wiesbaden, 2014.
- [4] I. Gibson, D. W. Rosen, and B. Stucker, *Additive Manufacturing Technologies: Rapid Prototyping to Direct Digital Manufacturing*. Springer US, 2009.
- [5] K. Struebig, F. Diller, and T. C. Lueth, "Influence of Filling Strategies on the Tensile Strength and Anisotropic Properties of Droplet-Based 3D-Printed Parts," in *2018 IEEE International Conference on Robotics and Biomimetics (ROBIO)*, 12-15 Dec. 2018, pp. 14-20, doi: 10.1109/ROBIO.2018.8665190.
- [6] R. Wang, K.-j. Cheng, R. C. Advincula, and Q. Chen, "On the thermal processing and mechanical properties of 3D-printed poly(ether ether ketone)," *MRS Communications*, pp. 1-7, 2019, doi: 10.1557/mrc.2019.86.
- [7] M. Sobieraj and C. Rimnac, "Fracture, Fatigue, and Notch Behavior of PEEK," 2012, pp. 61-73.
- [8] C. Hopmann, "Rettungsschirm für gebrochene Herzen," *Kunststoffe*, vol. 9/2013, pp. 184-187, 2013.
- [9] M. Vaezi and S. Yang, "Extrusion-based additive manufacturing of PEEK for biomedical applications," *Virtual and Physical Prototyping*, vol. 10, pp. 1-13, 10/13 2015, doi: 10.1080/17452759.2015.1097053.
- [10] A. Schröffer, J. Prsa, F. Irlinger, and T. C. Lüth, "A novel building strategy to reduce warpage in droplet-based additive manufacturing of semi-crystalline polymers," in *2018 IEEE International Conference on Robotics and Biomimetics (ROBIO)*, 12-15 Dec. 2018, pp. 1894-1899, doi: 10.1109/ROBIO.2018.8665054.
- [11] C. Yang, X. Tian, D. Li, Y. Cao, F. Zhao, and C. Shi, "Influence of thermal processing conditions in 3D printing on the crystallinity and mechanical properties of PEEK material," *Journal of Materials Processing Technology*, vol. 248, pp. 1-7, 2017/10/01/ 2017, doi: <https://doi.org/10.1016/j.jmatprotec.2017.04.027>.
- [12] L. Jin, J. Ball, T. Bremner, and H.-J. Sue, "Crystallization behavior and morphological characterization of poly(ether ether ketone)," *Polymer*, vol. 55, pp. 09/01 2014, doi: 10.1016/j.polymer.2014.08.045.